

POLITECNICO DI TORINO

---

Electronic and Communications Engineering



---

## Assignment Report 7 - Array signal processing

---

Applied Signal Processing Laboratory

01TUMLP

Academic Year 2019/20

Gloria DAL SANTO  
s245220

# Exercise 1

In this exercise it was required to analyze some examples of Conventional Beamforming (CB) for Uniform Linear Array (ULA).

The given parameters of the first configuration were the number of antennas  $N = 8$ , the carrier frequency of the impinging signal  $f_c = 900\text{MHz}$  and its Direction of Arrival (DoA)  $\theta_1 = 0^\circ$ . Approximating the speed of light to  $c = 3 \cdot 10^8 \text{m/s}$ , the wavelength of the signal is  $\lambda = c/f_c \approx 0.33\text{m}$ . I set the distance between two consecutive antennas to be  $d = \lambda/2$ , the limit value that satisfies the sampling theorem. With this initial parameters, I computed the ULA pattern  $\mathbf{V}(\theta)$ , for a set of  $S = 3601$  equally spaced values of the angle  $\theta$ , and the beamformer  $\mathbf{w} = \mathbf{a}(\theta_1)/\sqrt{N}$ . Finally I obtained the Array Factor (AF) as  $\mathbf{w}^H \mathbf{V}(\theta)$ . Figure 1 shows the magnitude of the obtained pattern, compared with that of the following dirichlet function:

$$|AF| = \frac{\sin(\frac{N}{2}\Psi)}{\sin(\frac{1}{2}\Psi)}$$

$$\Psi = 2\pi \frac{d}{\lambda} (\sin\theta - \sin\theta_1)$$
(1)

It can be seen that the AF and eq.(1) end up to the same result.

Then I applied eq.(1) to obtain the AFs of four ULA configurations with same intial  $\theta_1$  and distance  $d$  but with a different number of antennas. Figure 2 depicts the four configurations and their corresponding value of  $N$ . It can be verified that the maximum value of each pattern is  $\sqrt{N}$ .

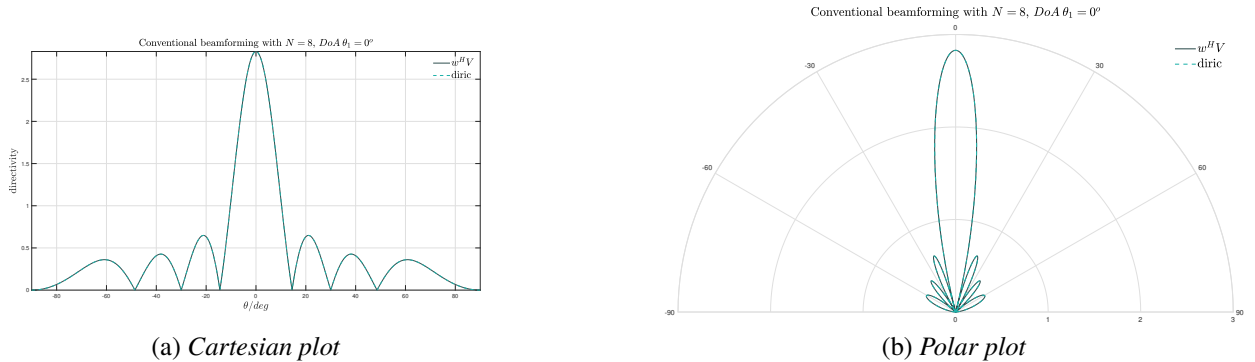


Figure 1: Exercise 1 - Array Factor of a CB configuration with  $N = 8$  and  $\text{DoA } \theta_1 = 0^\circ$ .

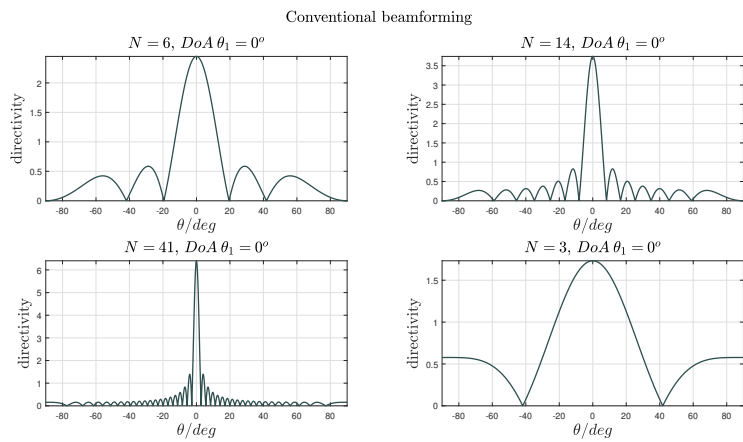


Figure 2: Exercise 1 - AF of different CB configurations with  $\text{DoA } \theta_1 = 0^\circ$  and  $N = 6, 14, 41, 3$ .

Figure 3 illustrates four more configurations, with  $N = 8$ ,  $\theta_1 = 0^\circ$  and  $d/\lambda = 0.25, 0.5, 1, 2$ . In the first two cases, the value of  $d/\lambda$  satisfies the sampling theorem and consequently the maxima of the array factor, evaluated with eq.(2), are located at  $\theta_1 = 0^\circ$ . For  $d/\lambda = 1$  and 2, aliasing effect occurs and it can be seen that secondary main lobes show up with maxima at  $\theta = 90^\circ$  and  $\theta = 30^\circ, 90^\circ$ , respectively.

$$\theta_n^{MAX} = \arcsin\left(\sin\theta_1 + m \frac{\lambda}{d}\right) \quad m = 0, 1, 2, \dots \quad (2)$$

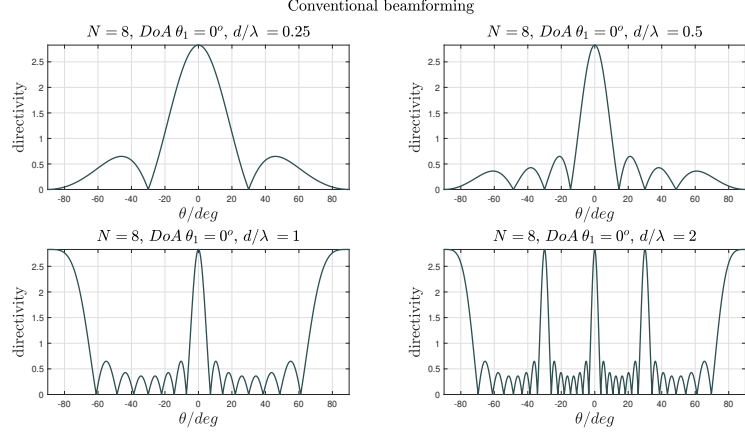


Figure 3: Exercise 1 - Sampling theorem effect on conventional beamforming

For the case of a ULA with 8 antennas, solving eq.(3) with  $n = 7$  and imposing  $\theta_n^{NULL} = 90^\circ$  I found that in order to get a pattern with maximum directivity, the distance  $d$  must be so that  $d/\lambda = 7/8$  (Figure 4). Since the array has 8 antennas, increasing  $n$  to a value higher than  $N - 1 = 7$  will cause the generation of grating lobes.

$$\theta_n^{NULL} = \arcsin\left(\sin\theta_1 + \frac{n}{N} \frac{\lambda}{d}\right) \quad n = 1, 2, \dots \quad n \neq N, 2N, 3N, \dots \quad (3)$$

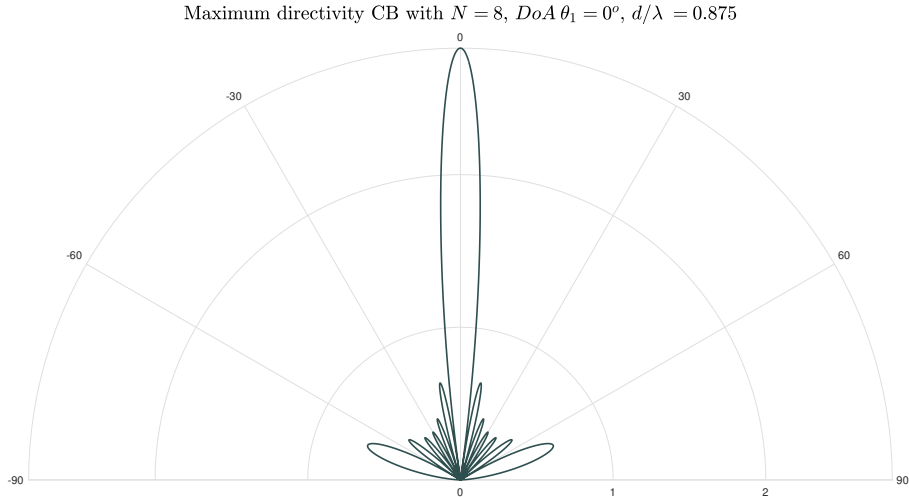


Figure 4: Exercise 1 - CB pattern with maximum directivity

Finally, for the case with  $N = 8$ ,  $d/\lambda = 0.5$  and  $\theta_1 = 30^\circ$  I computed the First Null Beam Width  $\Delta\theta = |\theta_1^{NULL} - \theta_{-1}^{NULL}|$  applying eq.(3) and I obtained  $FNBW \approx 34.11^\circ$ . Then, recurring again to eq.(3) I found that for  $\theta_1 = 60^\circ$  the minimum  $N$  that ensures the first null to be at  $\theta_1 < 90^\circ$  is  $N = 15$ , for which we have that  $\theta_1 \approx 87.95^\circ$  (Figure 5).

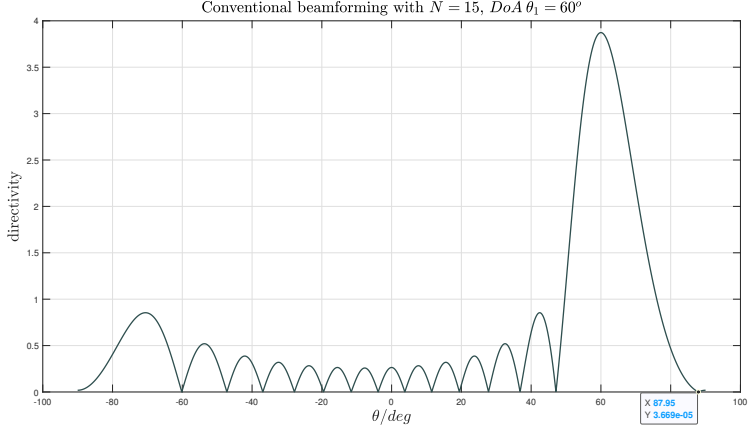


Figure 5: Exercise 1 - *Conventional beamforming pattern with  $N = 15$*

## Exercise 2

In this exercise I used the same initial ULA parameters of the previous exercise, with the addition of five interferers whose DoAs are  $\theta_I = [20^\circ, -40^\circ, 60^\circ, -75^\circ, 80^\circ]$  and in the presence of noise with variance  $\sigma_n^2 = 10^{-5}$ . I computed the Capon beamformer  $\mathbf{w}_{MVDR}$  as follows:

$$\mathbf{w}_{MVDR} = \frac{\mathbf{R}_y^{-1}\mathbf{a}(\theta_1)}{\mathbf{a}^H(\theta_1)\mathbf{R}_y^{-1}\mathbf{a}(\theta_1)} \quad (4)$$

where the interference plus noise covariance matrix  $\mathbf{R}_y^{-1}$  is defined as  $\mathbf{R}_y^{-1} = \mathbf{A}(\theta_I)\mathbf{A}(\theta_I)^H + \sigma_n^2\mathbf{I}$  (assuming that the signal has unitary  $\sigma_s^2$ ).

Reusing the code of the first exercise that generates the array pattern  $\mathbf{V}(\theta)$ , I derived the Array Factor  $\mathbf{w}_{MVDR}^H \mathbf{V}$ , obtaining the configuration depicted in Figure 6. It can be seen that the pattern takes minimum values at the DoA of the interferers, as wanted. Figure 7.(a) and (b) show two similar scenarios were the DoA of the first interferer is changed to  $\theta_{I1} = 10^\circ$  and  $\theta_{I1} = 5^\circ$ , respectively.

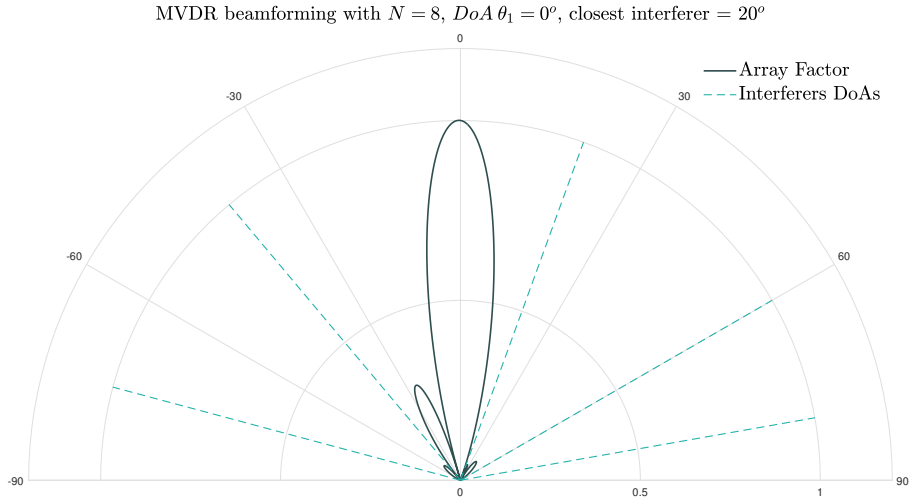


Figure 6: Exercise 2 - *Capon beamforming with closest interferer at  $\theta = 20^\circ$*

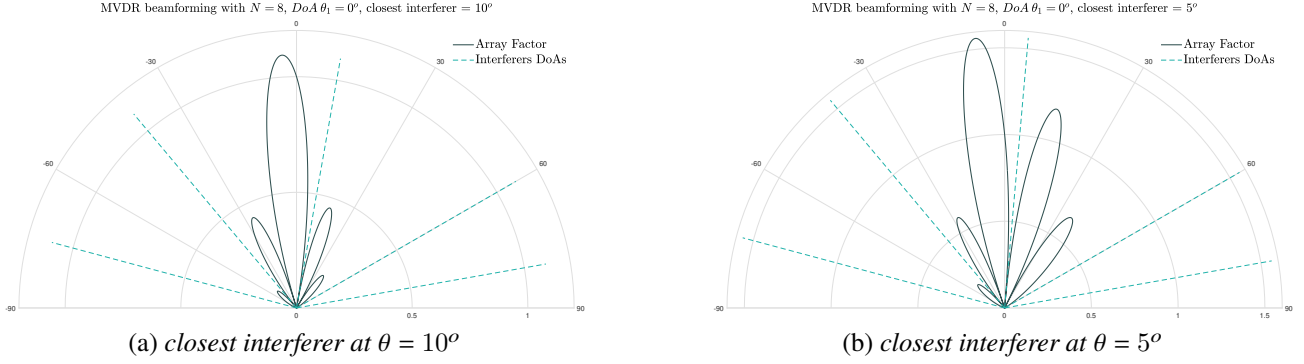


Figure 7: Exercise 2 - *Capon beamforming*

Figure 8 compares the Array Factors obtained with Capon beamforming and conventional beamforming in the case of 31 interferers with equally spaced DoAs along  $\theta$ . I obtained the number of nulls and the corresponding angles applying the formula in eq.(3), setting the last nulls at  $\pm 90^\circ$ . The resulting  $\theta_n^{NULL}$  are  $\pm 14.48^\circ$ ,  $\pm 30^\circ$ ,  $\pm 48.59^\circ$ ,  $\pm 90^\circ$ . Even if in the plot the directivities of the main lobes are very similar, it can be seen that the Capon beamformer gives smaller side lobes compared to those of the conventional beamformer. Apart from this there are no other relevant differences, the Capon beamformer simply cannot minimize the interferences coming from all the DoAs. For an increasing number of interferers the optimal beamformer appears to be the conventional one.

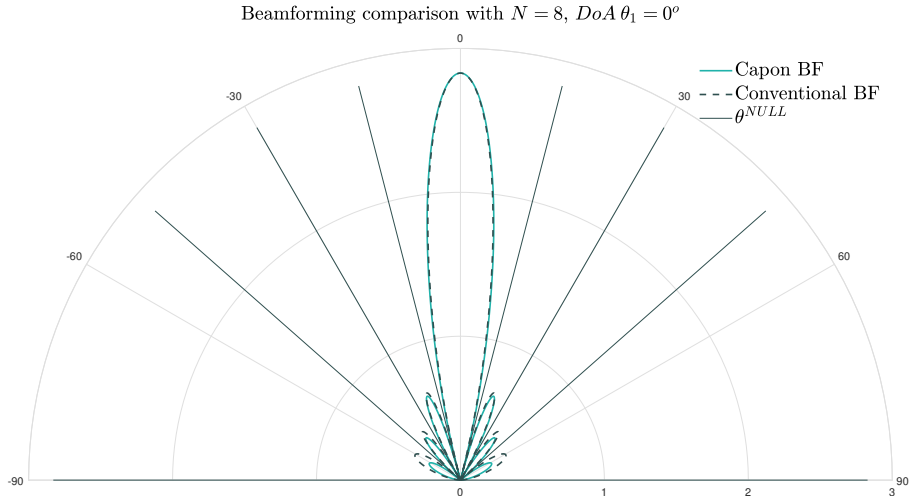


Figure 8: Exercise 2 - *Array Factor comparison between Capon and conventional beamforming*

## Exercise 3

In this exercise it was required to analyze the conventional beamforming with Uniform Planar Array (UPA) arrangement with directive antenna elements characterized by the following directivity function:

$$d(\theta, \phi) = 0.25 \cdot [1 - \cos(2 \cdot \theta)] \cdot [1 + \cos(\phi)] \quad (5)$$

Using the UPA arrangement, the beam can be steered along both the azimuth and elevation angles and the conventional beamforming can be defined as in eq.(6) where  $(\theta_1, \phi_1)$  corresponds to the DoA of

the user.  $N_z$  is the number of elements along  $z$  and  $N_y$  is the number of elements along  $y$ .

$$\mathbf{w} = \frac{1}{\sqrt{N_z N_y}} \mathbf{a}(\theta_1, \phi_1) \quad (6)$$

In this exercise, the UPA has dimension 8x8 with antennas spaced 0.025 along both  $z$  and  $y$  axis. Figures 9.(a) and (b) show the pattern  $\mathbf{w}^H \mathbf{A}(\theta, \phi)$  where  $\mathbf{w}$  is set to compensate for the DoA ( $100^\circ, 30^\circ$ ). The pattern in Figure 9.(a), being composed of isotropic antenna elements, has the main lobe along the DoA and also an unwanted grating lobe of the same size along ( $100^\circ, 150^\circ$ ). The directive antenna elements used in the case illustrated in Figure 9.(b), and characterized by eq.(5), are extended mainly in the positive  $x$  axis ( $270^\circ < \phi < 90^\circ$ ). As a consequence the resulting UPA pattern has no secondary main lobe, ensuring that the gain of the array is concentrated in the desired DoA. Figures 10 and 11 illustrate the case of DoA ( $105^\circ, 30^\circ$ ) and DoA ( $70^\circ, -45^\circ$ ), respectively.

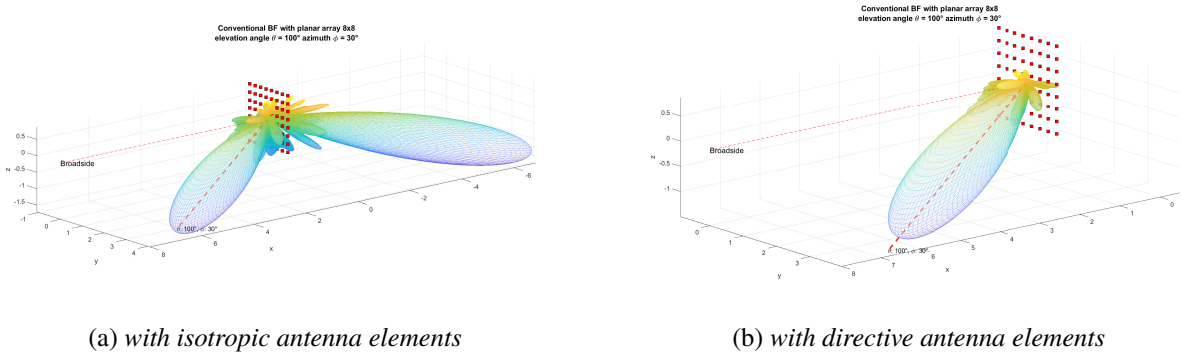


Figure 9: Exercise 3 - *Conventional beamforming, DoA ( $100^\circ, 30^\circ$ )*

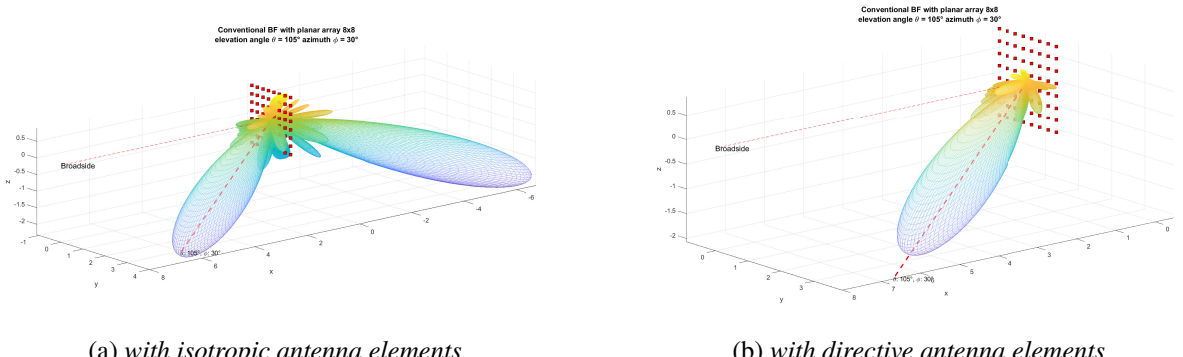
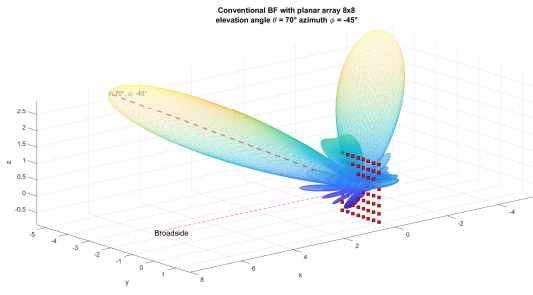
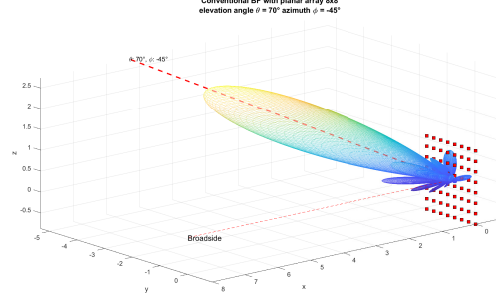


Figure 10: Exercise 3 - *Conventional beamforming, DoA ( $105^\circ, 30^\circ$ )*

Figure 12 depicts the case of an antenna array with dimensions  $32 \times 4$  and DoA ( $100^\circ, 60^\circ$ ). The resulting UPA pattern is different from the previous ones. Since the array has no equal dimensions, the main lobe is flatter than in the previous case, and it extends along the elevation angle. Moreover, there are no nulls that separate it from the grating lobe centered at ( $100^\circ, 120^\circ$ ) which is still present even if the directive antenna elements are applied (Figure 12.(b)).

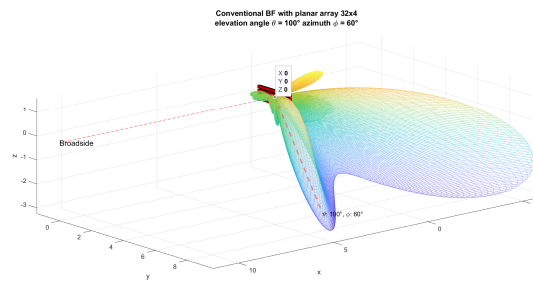


(a) with isotropic antenna elements

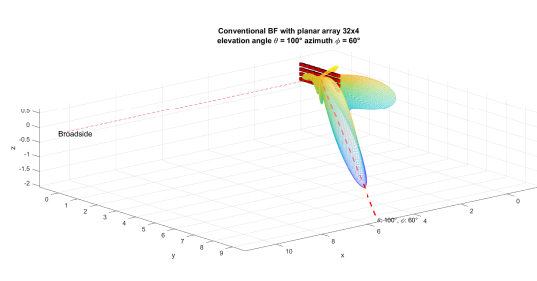


(b) with directive antenna elements

Figure 11: Exercise 3 - Conventional beamforming, DoA ( $70^\circ, -45^\circ$ )



(a) with isotropic antenna elements



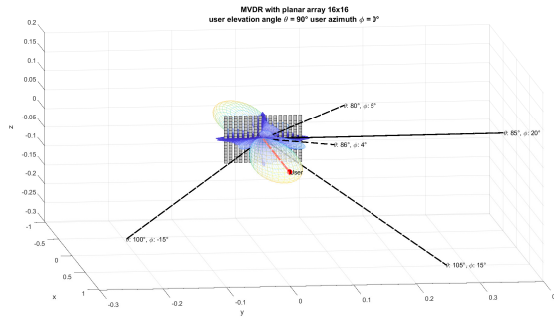
(b) with directive antenna elements

Figure 12: Exercise 3 - Conventional beamforming 32x4, DoA ( $100^\circ, 60^\circ$ )

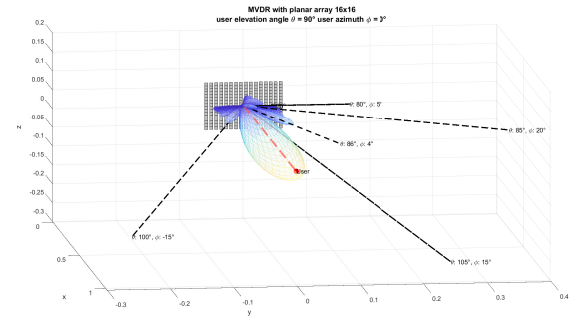
## Exercise 4

This last exercise asked to analyze the pattern of a Capon beamformer with a UPA arrangement of  $16 \times 16$  antenna elements. The beamformer is defined as in eq.(4) where the steering vector  $\mathbf{a}$  now depends also on  $\phi$ .

The interferers' DoAs are defined as  $(\theta, \phi) = [(86^\circ, 4^\circ), (85^\circ, 20^\circ), (80^\circ, 5^\circ), (100^\circ, -15^\circ), (105^\circ, 15^\circ)]$ , the noise variance is  $\sigma_n^2 = 10^{-5}$  and the power related to the interferes is set to 1. With these parameters and for the DoA of the user  $(\theta_1, \phi_1) = (90^\circ, 0^\circ)$ , the resulting patterns are those depicted in Figure 13.(a) and (b), respectively for isotropic and directive antenna elements.



(a) with isotropic antenna elements



(b) with directive antenna elements

Figure 13: Exercise 4 - Capon beamforming, DoA ( $90^\circ, 0^\circ$ )

Also in this case the effect of the directive antenna is that of reducing the lobes along the negative  $x$  axis. Looking at the base of the pattern, it can be seen that all the interferers' DoAs correspond to a null, as it was expected from the Capon beamformer.

Figure 14 refers to the same configuration, with the DoA of the first interferer moved to  $(88^\circ, 2^\circ)$ .

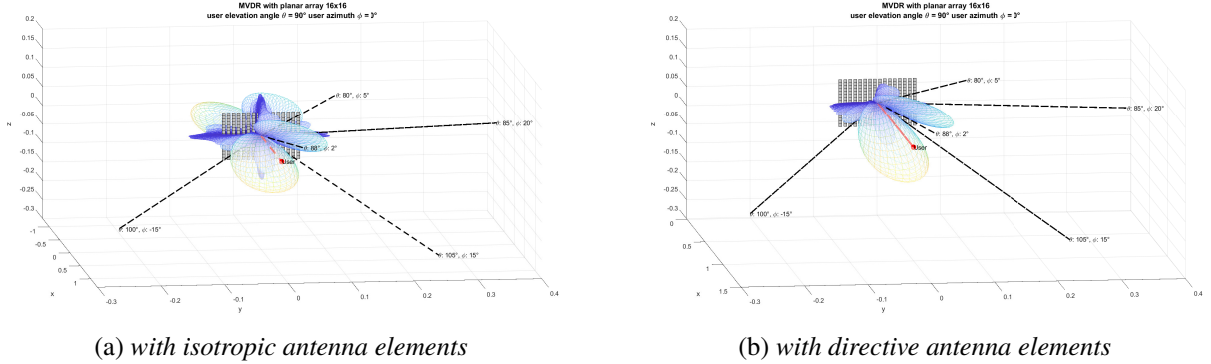


Figure 14: Exercise 4 - MVDR beamforming, DoA  $(90^\circ, 0^\circ)$ , DoA<sub>1</sub> $(88^\circ, 2^\circ)$

In this case the directions of the user and the first interferer are closer, resulting to a greater secondary lobe located approximately between the first and the third interferers. Also the other side lobes appear to have a greater amplitude.

Finally, I first tested the beamformer for a noise variance  $\sigma_n^2 = 1$  but then, since the pattern did not change at all, I increased it to  $\sigma_n^2 = 100$  only to see appreciable differences. The magnitude of the main lobe decreased from 1.3 to 1 and its central axis tilted from a slightly sloping direction to a precisely perpendicular position w.r.t the  $yz$  plane (alligned with the user's DoA). Moreover, all the grating lobes reduced to more symmetric side lobes. As a consequence of these two changes, the path covered by the nearest interferer falls inside the main lobe and thus its effect on the received signal will no more minimized (Figure 15). Comparing the pattern with that generated with the conventional beamformer, for the same array and user's DoA, it can be seen that they look approximately the same. In conclusion, I can say that the Capon beamformer can optimize the pattern, given a set of interferers DoAs, only in presence of relative small noise. On the other hand if the noise increases it will eventually converge to the pattern generated with the conventional beamformer in order to reduce the effect of the noise, present in all directions.

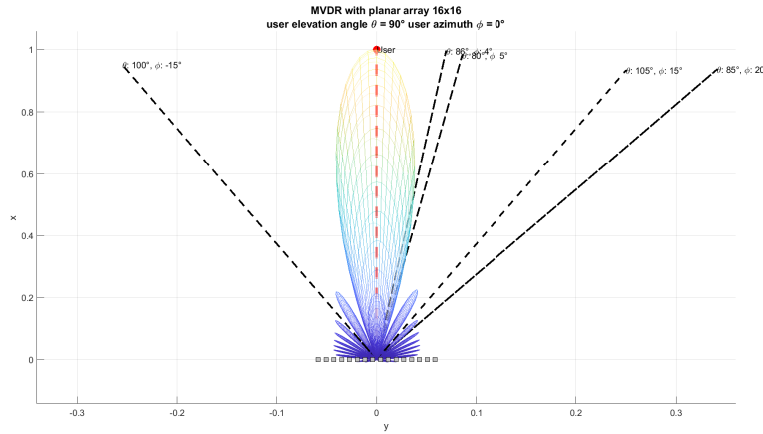


Figure 15: Exercise 4 - MVDR beamformer with  $\sigma_n^2 = 100$